RESEARCH ARTICLE
doi: 10.2306/scienceasia1513-1874.2015.41.042

ScienceAsia 41 (2015): **42–48**

Sm/N-codoped TiO_2 preparation, characterization, and photocatalytic decolourization of Acid Orange 7 and Basic Blue 41 in sunlight

Wisit Hirunpinyopas[a], **Sean A. Davis**[b], **Weekit Sirisaksoontorn**[a], **Apisit Songsasen**[a,*]

[a] Department of Chemistry and Centre of Excellence for Innovation in Chemistry, Faculty of Science, Kasetsart University, Latyao, Chatuchak, Bangkok 10900 Thailand
[b] School of Chemistry, University of Bristol, Bristol BS8 1TS, UK

*Corresponding author, e-mail: e-mail:fsciass@ku.ac.th

Received 18 Sep 2014
Accepted 15 Feb 2015

ABSTRACT: A Sm/N-codoped TiO_2 photocatalyst was successfully prepared via a sol-gel method using ammonium hydroxide and samarium(III) acetylacetonate as nitrogen and samarium sources, respectively. The anatase phase of TiO_2 was mainly observed in a Sm/N-codoped product calcined at 500 °C as indicated by the X-ray diffraction pattern. The crystallite size of Sm/N-codoped TiO_2 ranged from 6–10 nm with a surface area (S_{BET}) of 109–155 m^2/g. Photoelectron spectroscopic results confirmed the incorporation of both Sm and N species into the TiO_2 structure, which substantially lowered the band gap energy of TiO_2. The photocatalyst activities were evaluated by the ability to decolourize solutions containing the organic azo dyes (i.e., AO7 and BB41) in sunlight. Sm/N-codoped TiO_2 calcined at 500 °C shows higher decolourization of AO7 than any other doped TiO_2 calcined at 500 °C, including undoped TiO_2. Interestingly, Sm-doped TiO_2 calcined at 400 °C could most efficiently decolourize AO7. For the decolourization of BB41 dye, N-doped TiO_2 calcined at 500 °C showed the highest photocatalytic efficiency.

KEYWORDS: photocatalyst, organic dyes

INTRODUCTION

TiO_2 is widely used as a photocatalyst due to its remarkable stability, easy availability, low toxicity, and outstanding photocatalytic activity[1,2]. In general, TiO_2 has three structural phases; anatase, brookite, and rutile, but the anatase phase has interestingly been shown for photodegradation activities because of its suitable band gap energy (3.2 eV)[3]. The photocatalytic activity of TiO_2 can be explained by the separation of electron-hole pairs occurring at TiO_2 surface. Typically, electrons (e^-) and positive holes (h^+) are generated by irradiation of light with an appropriate photon energy corresponding to the band gap of TiO_2. The electrons can be excited into the conduction band after irradiated with light and positive holes still stay in the valence band. Subsequently, both species can migrate to the TiO_2 surface. The photogenerated electrons directly react with O_2 molecules adsorbed on the TiO_2 surface, to form superoxide radicals $O_2^{-\cdot}$ which further react with free protons (H^+) to produce H_2O_2. On the contrary, the positive holes react with H_2O molecules or hydroxyl groups to generate hydroxyl radicals ($HO^\cdot$) which are mainly involved in the degradation process[3–5].

Generally, TiO_2 is photocatalytically active only under the UV light due to its large band gap of 3.0 eV for rutile and 3.2 eV for anatase. Since sunlight primarily consists of visible wavelengths, i.e., very small portion of the UV light, many have attempted to decrease the TiO_2 band gap in order that TiO_2 can absorb light in a visible region. In the present study, chemical substitution is a promising way by, for example, replacing some oxygen atoms with nitrogen atoms[3]. This mixed state of N 2p and O 2p can lower the band gap of TiO_2. Although the electrons can be excited from the valence band by photon energy, the recombination process is still so rapid within 50 ± 30 ns for the lifetime on anatase (001)[4]. This results in the reduction of photocatalytic efficiency of TiO_2. Samarium (Sm) is a rare earth element widely used as a supporting catalyst due to its unique electronic configuration

(occupied 4f orbitals and empty 5d orbitals)[5–8]. The energy level of 4f orbitals of Sm^{3+} is between the energy level of the valence and conduction bands of TiO_2. Hence Sm can be used as a dopant to enhance the electronic transition and suppress the e^--h^+ pair recombination[7–9]. Thermally stable Sm/N-codoped TiO_2 has been prepared using coprecipitation method in order to degrade salicylic acid under visible light irradiation. The photocatalytic activity of the codoped TiO_2 was higher than N-doped TiO_2 and pure TiO_2[8].

A wide variety of organic dyes, including heteroaromatic compounds containing azo groups ($-N=N-$) or other auxochromes (OH^-, SO_3^-, NH_2, etc.), are used in industry, finding uses in cosmetics, tanning, printing, and clothing applications[10]. In particular, azo dyes can be divided into two main types, acidic (anionic dye) and basic (cationic dye) dyes. These dyes are of considerable interest because they are toxic, nonbiodegradable, carcinogenic, and mutagenic[11,12]. Methods for their degradation are also widely discussed[13–15].

In this work, TiO_2 photocatalysts doped with Sm, N, and codoped with Sm/N were prepared by using the sol-gel method. The nanostructure and morphology of photocatalysts were characterized using a variety of analytical methods. The effects of calcination temperature and Sm/N doping on the decolourization efficiency were studied. The typical anionic azo dye, AO7, and cationic azo dye, BB41, were used to determine the efficiency of the prepared photocatalysts under the sunlight.

MATERIALS AND METHODS

Photocatalyst preparation

Sm/N-codoped TiO_2 was prepared by the sol-gel method. Initially, 0.76 g (14% w/w of Ti) of samarium(III) acetylacetonate hydrate was dissolved in a mixture of 3 ml of acetylacetone and 10 ml of ethylene glycol under a constant stirring rate (400 rpm) at room temperature. Then 10 ml of titanium(IV) isopropoxide was added to the mixture until the temperature of the exothermic process reached room temperature. In the second step, 5 ml of 30% NH_4OH solution was added dropwise and the mixture was stirred until a yellow gel was formed. After that the xerogel was aged for 12 h and heated at 120 °C for 4 h. The as-prepared Sm/N-codoped TiO_2 was calcined in a muffle furnace at 400 and 500 °C for 2 h. For comparison, Sm-doped TiO_2, N-doped TiO_2, and undoped TiO_2 photocatalysts were also prepared using the same procedure.

Photocatalyst characterization

The crystalline phase of the photocatalysts was determined by X-ray diffraction (XRD, Philips X-Pert) operated at 40 kV and 30 mA using nickel-filtered Cu K_α radiation ($\lambda = 1.54$ Å). The crystallite size was determined from the full width at half maximum peak breadth using Scherrer's equation[16]. The Brunauer-Emmett-Teller (BET) specific surface area and pore size distribution were determined by N_2 adsorption (Quantachrome instrument model ASIC-2 with Autosorp-1 program). The morphology of the catalysts was determined using a Scanning electron microscope (SEM, JEOL JSE-5600Lv). The particle sizes and the lattice fringes were determined by Transmission electron microscope (TEM, JEOL 1200-EX II). The UV-Vis absorption spectra of catalysts were obtained by mounting the prepared samples on a glass plate, using acetone to aid adherence, with a Diffuse Reflectance UV-Vis spectrophotometer (UV-Vis-DRS, Perkin Elmer Lambda 650). The Raman shifts of the doped and undoped TiO_2 was recorded on a Renishaw Raman Imaging Microscope with green laser ($\lambda = 633$ nm). The photoemission spectroscopy (PES) technique was performed at the Siam Photon Laboratory (Synchrotron Light Research Institute, Nakhon Ratchasima, Thailand) using a VG Scientific concentric hemispherical analyser with a Synchrotron radiation source. All the peaks were referenced to the O Auger and C 1s peaks at 85.75 and 283.75 eV, respectively.

Photocatalytic activity measurements

The photocatalytic activities were evaluated based on the extent of decolourization of azo dyes (AO7 and BB41) in an aqueous solution. The initial concentration of azo dye was 20 mg/l. The amount of catalysts added to the solution was 0.10 g/100 ml. The decolourization reaction was performed for 6 h under the sunlight (30–33 °C). The decolourization of azo dyes were monitored by measuring the concentration change of azo dyes via a UV-Vis spectrophotometer (Perkin Elmer Lambda 35) at fixed wavelengths of 484 and 617 nm for AO7 and BB41, respectively. The decolourization η was calculated as

$$\eta = \frac{C_0 - C_t}{C_0}$$

where C_0 and C_t are the concentrations of azo dyes at the initial time point and after the reaction, respectively. All experiments were conducted in triplicate.

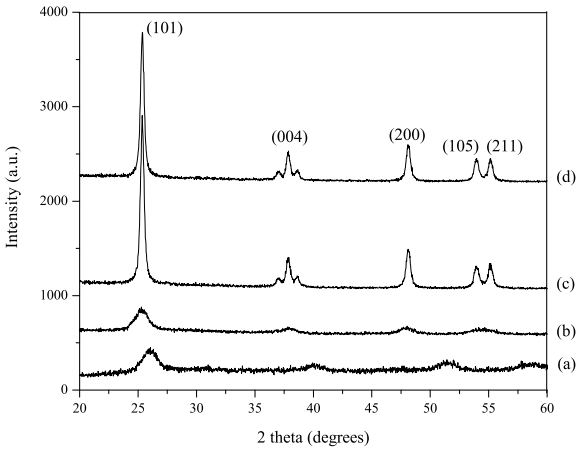

Fig. 1 The XRD patterns of the as-prepared TiO_2 photocatalysts calcined at 500 °C. (a) Sm/N-TiO_2, (b) Sm-TiO_2, (c) N-TiO_2, and (d) undoped TiO_2.

RESULTS AND DISCUSSION

Characterization of photocatalysts

Fig. 1 shows the X-ray diffraction patterns of the prepared catalysts calcined at 500 °C. For the two different calcination temperatures, the anatase phase was predominately observed at 2θ of 25.6°, 38.1°, 48.2°, 54.0°, and 55.5°, corresponding to the standard XRD pattern (JCPDS files No. 21-1272). It is worth to note that all TiO_2 calcined at 500 °C did not exhibit any rutile peak. In addition, the crystallinity of Sm/N-TiO_2 and Sm-TiO_2 are less than N-TiO_2 and undoped TiO_2 which is due to the doping of Sm into TiO_2 lattice that retarded amorphous to anatase phase transformation. The crystallite sizes of Sm/N-codoped TiO_2 calcined at 400 and 500 °C calculated from Sherrer's equation[16] were 6.4 and 8.6 nm, respectively (Table 1). This result suggests that the crystallite size increases with an increasing calcination temperature. N-doped TiO_2 and undoped TiO_2 show larger crystallite sizes compared to TiO_2 containing Sm as a dopant (Table 1). This is due to the effect of Sm doping that can efficiently prevent the process of crystal growth[6]. Moreover, the unit cell volume of Sm/N-codoped TiO_2 did not significantly change when increasing the calcination temperature (130.8 $Å^3$ at 400 °C and 128.7 $Å^3$ at 500 °C) (Table 1). The specific surface area (S_{BET}) of Sm/N-codoped TiO_2 calcined at 500 °C was 108.9 m^2/g less than that calcined at 400 °C (154.7 m^2/g) in Table 1. This indicates the effect of the greater agglomeration of catalyst particles with an increasing temperature. It is clearly seen

Table 1 The effect of calcination temperature (T_{cal}) on the crystallite size, unit cell volume, and surface area of Sm/N-codoped TiO_2, Sm-doped TiO_2, N-doped TiO_2, and undoped TiO_2.

Photocatalyst	T_{cal} (°C)	Crystallite size (nm)	Unit cell vol ($Å^3$)	S_{BET} (m^2/g)
Sm/N-TiO_2	400	6.37	130.8	154.7
	500	8.65	128.7	108.9
Sm-TiO_2	400	7.22	135.8	188.7
	500	8.35	136.2	113.8
N-TiO_2	400	11.32	136.0	253.7
	500	26.54	135.8	74.0
Undoped TiO_2	400	10.99	135.6	39.8
	500	25.56	135.8	13.0

that all doped TiO_2 samples show higher specific surface areas at both 400 and 500 °C calcination temperatures compared to undoped TiO_2 (Table 1). For the Sm/N-codoped TiO_2 calcined at 500 °C, the pore volume and average pore diameter were 0.117 cm^3/g and 42.80 Å, respectively; the pore size distributions calculated from the desorption branch of the N_2 isotherm by the Barrett-Joyner-Halenda method were in the range of 15–50 nm.

The Raman peak shifts of Sm/N-codoped TiO_2 calcined at 500 °C (Fig. 2) were observed at 399 cm^{-1} (B_{1g}), 518 cm^{-1} (A_{1g}/B_{1g}), and 640 cm^{-1} (E_g), all of which have been assigned to be Raman-active lattice vibrations in anatase phase of TiO_2[16–18]. The result supports XRD data that only anatase was formed in this sample without

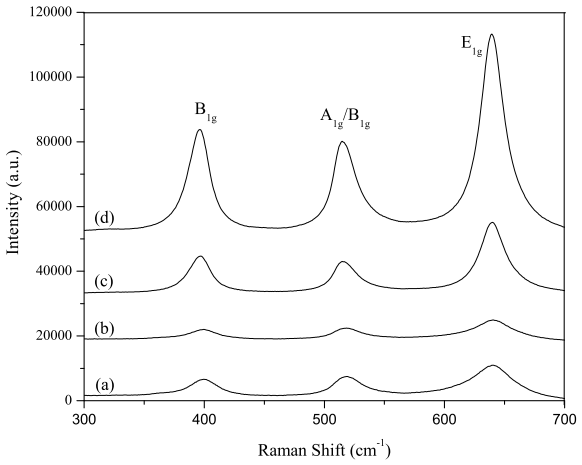

Fig. 2 Raman spectra of (a) Sm/N-codoped TiO_2, (b) Sm-doped TiO_2, (c) N-doped TiO_2, (d) undoped TiO_2. All catalysts were calcined at 500 °C.

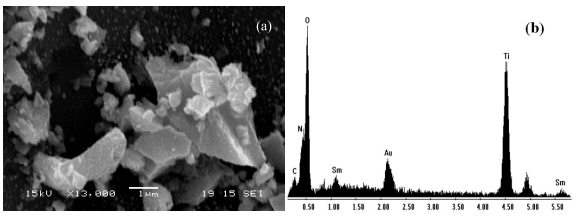

Fig. 3 (a) SEM and (b) EDS image of Sm/N-codoped TiO_2 calcined at 500 °C.

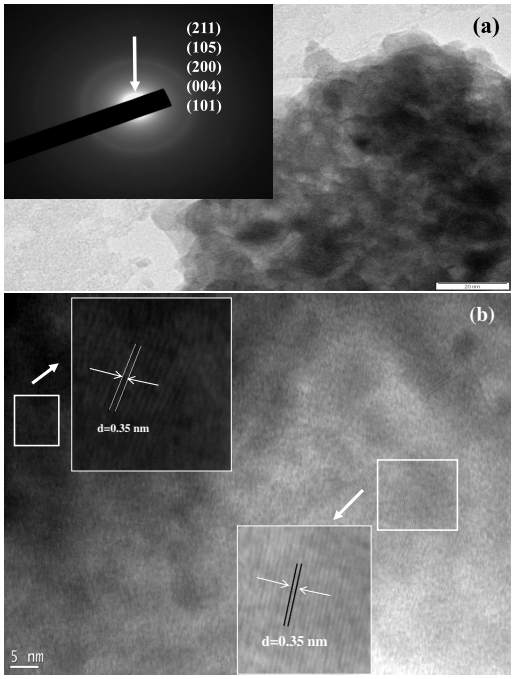

Fig. 4 (a) TEM and (b) HR-TEM images of the Sm/N-codoped TiO_2 calcined at 500 °C. The inset to (a) shows the corresponding selected area electron diffraction. The inset to (b) shows the corresponding *d*-spacing of the anatase phase.

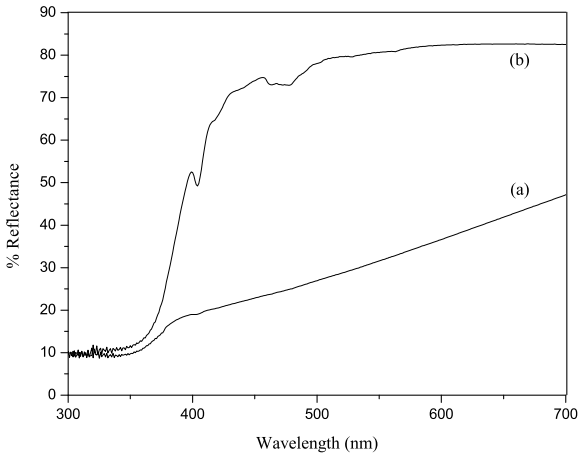

Fig. 5 Effect of calcination temperature on absorption edges of Sm/N-codoped TiO_2 calcined at (a) 400 °C, (b) 500 °C.

further phase transformation to rutile. In addition, the Raman peaks in Sm/N-codoped TiO_2 and Sm-doped TiO_2 calcined at 500 °C shifted to 518 cm^{-1} compared with 514 cm^{-1} in N-doped and undoped TiO_2 (Fig. 2). This is because of the doping effect of Sm^{3+} which causes the distortion in TiO_2 lattice corresponding to the bond of Sm—O—Ti[6,8,9].

The surface morphology of the Sm/N-codoped TiO_2 catalysts calcined at 500 °C was observed with the EDS-SEM spectrum in Fig. 3. The result clearly shows the presence of four obtained elements (Ti, O, N, and Sm) in this sample. The TEM image in Fig. 4a shows that the particle size of Sm/N-codoped TiO_2 is in the range of 6–10 nm (std.dev: 12 nm) which agrees well with the crystallite size calculated from the XRD data. The selected area electron diffraction image in the inset of Fig. 4a indicates that Sm/N-codoped TiO_2 calcined at 500 °C is in a pure anatase phase. HR-TEM image in Fig. 4b shows the high crystallinity of the TiO_2 particles with the lattice fringe (*d*-spacing) of 0.35 nm corresponding to the distance between (101) crystal planes of the anatase phase[16,19].

The UV-Vis DRS spectra of Sm/N-codoped TiO_2 calcined at 400 and 500 °C in Fig. 5 show absorption edges of 380 and 440 nm corresponds to the band gap energies of 3.26 and 2.81 eV, respectively, compared to that of pure undoped TiO_2 (3.10 eV)[8,20]. Thus both doping species and calcination temperature (i.e., especially at 500 °C) have a significant impact on the lowering of TiO_2 band gap energy[6,21]. This will enhance the photocatalytic activity of a photocatalyst under the sunlight. To further investigate all components of the Sm/N-codoped TiO_2 lattice, the PES technique was used to measure the binding energy of the Ti 2p, O 1s, N 1s and Sm 4d. The PES result of the Sm/N-codoped TiO_2 calcined at 400 °C shows the characteristic peaks of Ti^{4+} in TiO_2 at the binding energies of 457.75 eV (Ti $2p_{3/2}$) and 463.75 eV (Ti $2p_{1/2}$) as demonstrated in Fig. 6a. The O 1s peak was clearly seen at the binding energy of 529.75 eV, suggesting the presence of Ti—O bonds. The N 1s peak at 396.17 eV points to the existence of Ti—N bonds and the N 1s peak at 399.09 eV may be an N—N, N—O, or N—C bond[3,7]. For Sm doping species, the Sm 4d peak was observed at 120.29 eV corresponding to a Sm—O—Ti bond[8,9].

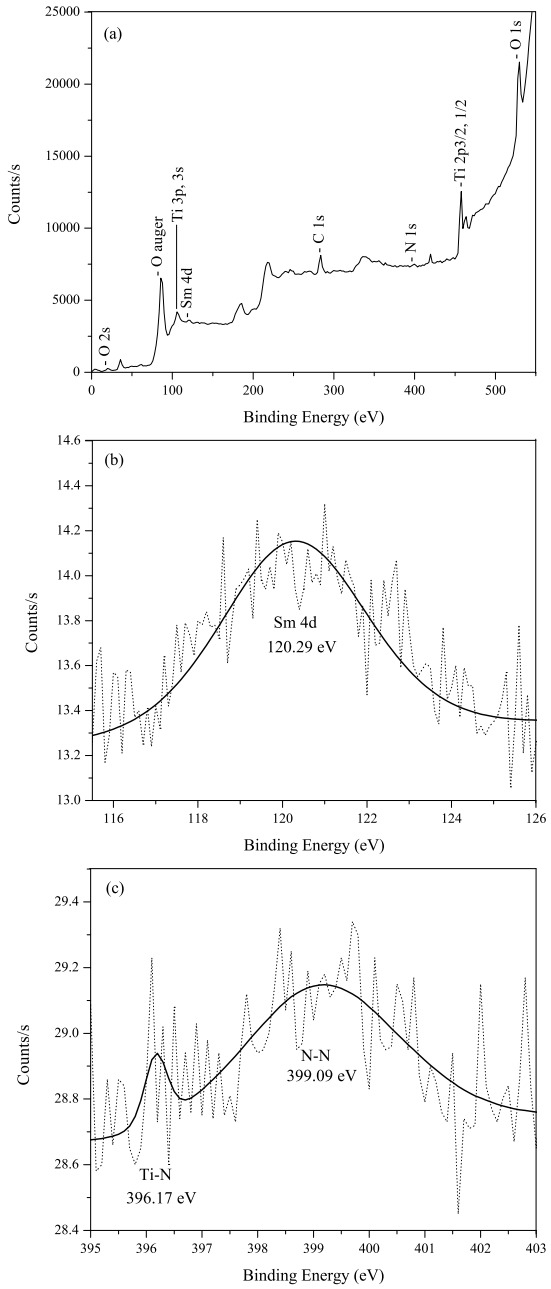

Fig. 6 (a) The survey PES spectrum of Sm/N-codoped TiO_2 calcined 400 °C, (b) Sm 4d and (c) N 1s.

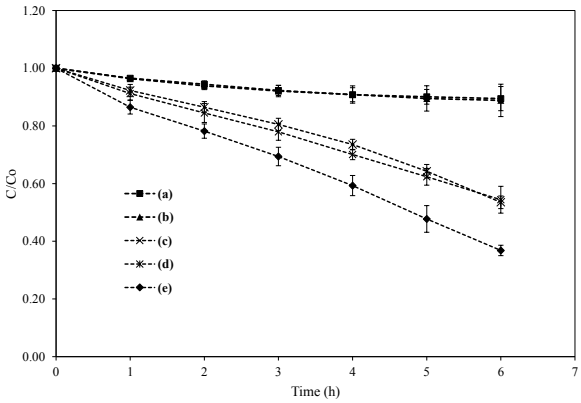

Fig. 7 Photocatalytic decolourization of AO7 under sunlight by (a) undoped TiO_2, (b) N-doped TiO_2, (c) Sm-doped TiO_2, (d) Sm/N-codoped TiO_2; all catalysts were calcined at 500 °C and (e) Sm-doped TiO_2 was calcined at 400 °C.

Table 2 Decolorization η and rate constant k of AO7 and BB41 under sunlight.

Photocatalyst	Calcination temp. (°C)	AO7		BB41	
		η (%)	k (h^{-1})	η (%)	k (h^{-1})
Sm/N-TiO_2	400	29	0.058	52	0.115
	500	46	0.099	24	0.040
Sm-TiO_2	400	63	0.160	62	0.159
	500	46	0.099	23	0.039
N-TiO_2	400	40	0.088	82	0.284
	500	11	0.019	83	0.267
Undoped TiO_2	400	43	0.097	38	0.080
	500	11	0.018	75	0.222

Photocatalytic activities

The photocatalytic activity of the Sm/N-codoped TiO_2 was studied in terms of its ability to decolourize the organic dye solution under the sunlight compared to Sm-doped TiO_2, N-doped TiO_2 and undoped TiO_2. For AO7, an anionic dye, the Sm/N-codoped TiO_2 calcined at 500 °C could decolourize AO7 with 46% decolourization and rate constant of 0.099 h^{-1} (Fig. 7), which is relatively more efficient than any other photocatalyst calcined at 500 °C (Table 2). Interestingly, the Sm-doped TiO_2 calcined at 400 °C shows even higher efficiency in decolourization (63%) with a rate constant of 0.160 h^{-1} compared to Sm/N-codoped TiO_2 calcined at 500 °C. This result can be described in terms of a higher specific surface area (188.7 m^2/g) and smaller crystallite size (7.22 nm). It is worth noting that Sm-doping and Sm/N-codoping species remarkably enhance the photocatalytic activity of TiO_2 to decolourize AO7 dye under the sunlight. For a cationic BB41 dye, however, the photocatalysts containing Sm as a dopant exhibits only 23% decolourization for Sm-doping and 24% decolourization for Sm/N-codoping (Fig. 8). Instead, N-doped

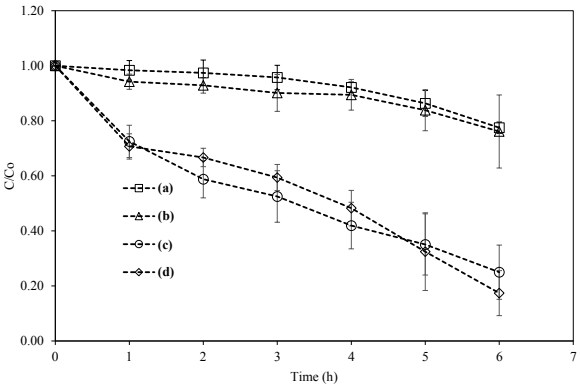

Fig. 8 Photocatalytic decolourization of BB41 under sunlight by (a) Sm-doped TiO_2, (b) Sm/N-codoped TiO_2, (c) undoped TiO_2 and (d) N-doped TiO_2. All catalysts were calcined at 500 °C.

TiO_2 calcined at 500 °C provided 83% decolourization of BB41 under the sunlight with the rate constant of 0.267 h^{-1}.

To elaborate the efficiency of TiO_2-based photocatalysts against the decolourization of an anionic AO7 and cationic BB41 dyes, the surface charge properties of doped TiO_2 is primarily taken into account. Typically, Sm-doping can increase the surface acidity of TiO_2 [22], which improves the amount of dyes, especially an anionic dye, adsorbed on TiO_2 surface. As a result, the AO7 dye was effectively decolourized by TiO_2 containing Sm dopants. On the contrary, N-doped TiO_2 with high basicity on its surface [23, 24] is strongly adsorbed by a cationic dye. Hence this N-doped TiO_2 showed the highest efficiency in decolourization of BB41 compared to others.

Conclusions

A relatively simple sol-gel method was successfully applied for the synthesis of nanoparticle Sm/N-codoped TiO_2. This photocatalyst was active for the decolourization of AO7 and BB41 under the sunlight. The as-prepared Sm/N-codoped TiO_2 calcined at 400 and 500 °C were both in the anatase phase as a result of Sm-doping effect that retards the phase transformation. The doping and calcination temperature effects cause the decrease in band gap energy of TiO_2. Depending on the surface charge nature of photocatalysts, Sm-doped and Sm/N-codoped TiO_2 show high photocatalytic efficiency on the AO7 decolourization. Meanwhile, N-doped TiO_2 strongly catalysed the decolourization of BB41 under the sunlight.

Acknowledgements: We would like to thank the Department of Chemistry, Kasetsart University and the Centre of Excellence for Innovation in Chemistry (PERCH-CIC), Office of the Higher Commission, Ministry of Education for financial support. We also thank the Siam Photon Laboratory Thailand for PES facility, the Development and Promotion of Science and Technology Talents (DPST) project for supporting grant, and Dr Paul Greeson for valuable suggestions.

REFERENCES

1. Chen C, Wang Z, Ruan S, Zou B, Zhao M, Wu F (2008) Photocatalytic degradation of C.I. Acid Orange 52 in the presence of Zn-doped TiO_2 prepared by a stearic acid gel method. *Dyes Pigments* **77**, 204–9.
2. Cao J, Xu B, Luo B, Lin H, Chen S (2011) Preparation, characterization and visible-light photocatalytic activity of AgI/AgCl/TiO_2. *Appl Surf Sci* **257**, 7083–9.
3. Sirisaksoontorn W, Thachepan S, Songsasen A (2009) Photodegradation of phenanthrene by N-doped TiO_2 photocatalyst. *J Environ Sci Health A* **44**, 841–6.
4. Ozawa K, Emori M, Yamamoto S, Yukawa R, Yamamoto S, Hobara R, Fujikawa K, Sakama H, Matsuda I (2014) Electron-hole recombination time at TiO_2 single-crystal surfaces: influence of surface band bending. *J Phys Chem Lett* **5**, 1953–7.
5. Shi Z, Yang X, Yao S (2012) Photocatalytic activity of cerium-doped mesoporous TiO_2 coated Fe_3O_4 magnetic composite under UV and visible light. *J Rare Earth* **30**, 355–60.
6. Xiao Q, Si Z, Yu Z, Qiu G (2008) Characterization and photocatalytic activity of Sm^{3+}-doped TiO_2 nanocrystalline prepared by low temperature combustion method. *J Alloy Compd* **450**, 426–31.
7. Huang DG, Liao SJ, Zhou WB, Quan SQ, Liu L, He ZJ, Wan JB (2009) Synthesis of samarium- and nitrogen-co-doped TiO_2 by modified hydrothermal method and its photocatalytic performance for the degradation of 4-chlorophenol. *J Phys Chem Solid* **70**, 853–9.
8. Ma Y, Zhang J, Tian B, Chen F, Wang L (2010) Synthesis and characterization of thermally stable Sm,N co-doped TiO_2 with highly visible light activity. *J Hazard Mater* **182**, 386–93.
9. Crepaldi EL, Soler-Illia GJAA, Grosso D, Cagnol F, Ribot F, Sanchez C (2003) Controlled formation of highly organized mesoporous titania thin films: from mesostructured hybrids to mesoporous nanoanatase TiO_2. *J Am Chem Soc* **125**, 9770–86.
10. Hammami S, Bellakhal N, Oturan N, Oturan MA, Dachraoui M (2008) Degradation of Acid Orange 7 by electrochemically generated ·OH radicals in acidic aqueous medium using a boron-doped diamond or

platinum anode: A mechanistic study. *Chemosphere* **73**, 678–84.
11. Chen X, Wang W, Xiao H, Hong C, Zhu F, Yao Y, Xue Z (2012) Accelerated TiO_2 photocatalytic degradation of Acid Orange 7 under visible light mediated by peroxymonosulfate. *Chem Eng J* **193-194**, 290–5.
12. Behnajady MA, Modirshahla N, Shokri M, Vahid B (2009) Design equation with mathematical kinetic modeling for photooxidative degradation of C.I. Acid Orange 7 in an annular continuous-flow photoreactor. *J Hazard Mater* **165**, 168–73.
13. Stylidi M, Kondarides DI, Verykios XE (2004) Visible light-induced photocatalytic degradation of Acid Orange 7 in aqueous TiO_2 suspensions. *Appl Catal B* **47**, 189–201.
14. Herney-Ramirez J, Silva AMT, Vicente MA, Costa CA, Madeira LM (2011) Degradation of Acid Orange 7 using a saponite-based catalyst in wet hydrogen peroxide oxidation: Kinetic study with the Fermi's equation. *Appl Catal B* **101**, 197–205.
15. Abbasi M, Asl NR (2008) Sonochemical degradation of Basic Blue 41 dye assisted by nano TiO_2 and H_2O_2. *J Hazard Mater* **153**, 942–7.
16. Orendorz A, Brodyanski A, Lösch J, Bai LH, Chen ZH, Le YK, Ziegler C, Gnaser H (2007) Phase transformation and particle growth in nanocrystalline anatase TiO_2 films analyzed by X-ray diffraction and Raman spectroscopy. *Surf Sci* **601**, 4390–4.
17. Sekiya T, Ohta S, Kamei S, Hanakawa M, Kurita S (2001) Raman spectroscopy and phase transition of anatase TiO_2 under pressure. *J Phys Chem Solid* **62**, 717–21.
18. Ma W, Lu Z, Zhang M (1998) Investigation of structure transformations in nanophase titanium dioxide by Raman spectroscopy. *Appl Phys A* **66**, 621–7.
19. Zhang Z, Wang X, Long J, Gu Q, Ding Z, Fu X (2010) Nitrogen-doped titanium dioxide visible light photocatalyst: Spectroscopic identification of photoactive centers. *J Catal* **276**, 201–14.
20. Ananpattarachai J, Kajitvichyanukul P, Seraphin S (2009) Visible light absorption ability and photocatalytic oxidation activity of various interstitial N-doped TiO_2 prepared from different nitrogen dopants. *J Hazard Mater* **168**, 253–61.
21. Di Valentin C, Finazzi E, Pacchioni G, Selloni A, Livraghi S, Paganini MC, Giamello E (2007) N-doped TiO_2: Theory and experiment. *Chem Phys* **339**, 44–56.
22. Rauf MA, Meetani MA, Hisaindee S (2011) An overview on the photocatalytic degradation of azo dyes in the presence of TiO_2 doped with selective transition metals. *Desalination* **276**, 13–27.
23. Jiang Y, Luo Y, Zhang F, Guo L, Ni L (2013) Equilibrium and kinetic studies of C.I. Basic Blue 41 adsorption onto N, F-codoped flower-like TiO_2 microspheres. *Appl Surf Sci* **273**, 448–56.
24. Miessler GL, Tarr DA (2004) *Inorganic Chemistry*, 3rd edn, Pearson Prentice Hall, Upper Saddle River, New Jersey, pp 179–92.